Technical Paper

ISSN 1997-1400 Int. J. Pavement Res. Technol. 8(6):403-409

Analysis of Loading Frequency in Flexible Pavement Using Fast Fourier Transform

Mohammad Hossein Shafiee [1], Arian Asefzadeh [1], Leila Hashemian [1], and Alireza Bayat [1+]

Abstract: Accurate calculation of traffic loading frequency plays a major role in mechanistic design of flexible pavements. Previous studies have highlighted the need for a paradigm shift in determining frequency through frequency domain analysis rather than conventional time domain-based methods. However, limited studies have experimentally investigated the impact of contributing factors including response type, depth and vehicle speed on calculated frequencies in frequency domain approach. This paper presents the results of controlled vehicle testing that focused on frequency analysis of in-situ measured pulses using Fast Fourier Transform (FFT). The tests were conducted in the Integrated Road Research Facility (IRRF) in Edmonton, Alberta, Canada. Longitudinal, transverse and vertical strains at the bottom of the Hot Mix Asphalt (HMA), as well as the vertical stresses recorded at different depths within unbound layers, were taken into account for this purpose. This study showed that dominant frequencies associated with longitudinal strain were the highest amongst those of other considered responses. Besides, the impact of speed and depths on obtained frequencies were clearly reflected. Finally, comparisons were made between the accuracy of HMA dynamic modulus prediction when using FFT-calculated frequency versus using of four well-established frequency calculation methods in time domain.

DOI: 10.6135/ijprt.org.tw/2015.8(6).403

Key words*: Dynamic modulus; Fast Fourier Transform; Loading frequency; Pavement response.*

Introduction

Hot Mix Asphalt (HMA) is a composite material whose viscoelastic behavior is highly dependent on temperature and loading frequency. It is well-documented in the literature that asphalt mix tends to exhibit linear behavior under lower temperatures and higher loading frequencies while its viscous behavior is more pronounced when it is subjected to higher temperatures and lower loading frequencies [1]. According to Mechanistic- Empirical Pavement Design Guide (MEPDG) [2], it is crucial to experimentally characterize the viscoelastic behavior of HMA by developing a master curve for HMA dynamic modulus, |E*|, through frequency sweep tests at different temperatures. It is also known that |E*| master curve is determined in the lab in frequency domain, while pavement is in fact subjected to the moving vehicles in time domain. As a result, various researchers have investigated different time-to-frequency conversion methods to accurately calculate the related frequency from traffic-induced stress or strain pulse duration [2-4]. Among these conversion approaches, the relations $f=1/t$ and $f=1/2\pi t$, where f is the frequency in Hz and t is time in s, are widely utilized for frequency calculation. For instance, the MPEDG adopts Odemark [5] approach to find the pulse duration and converts it to frequency using the relation $f=1/t$. However, recent studies have shown that the direct use of response pulse duration and converting it to frequency based on aforementioned methods in time domain can result in erroneous estimation of frequencies which can consequently affect the |E*| [6, 7]. Al-Qadi *et al.* [6] examined the accuracy of the MEPDG's frequency calculation method with respect to the frequencies obtained from Fast Fourier Transform (FFT) in frequency domain at the Virginia Smart Road. Using stress pulses recorded at two different depths under three vehicle speeds of 8, 24 and 40 km/hr, frequencies obtained based on the MEPDG method were more than 2 times larger than those of FFT method. This study showed that using Odemark approach and conventional time-to-frequency conversion method are the possible sources of error when finding frequency in time domain.

In addition, vehicular loading induces different pulses across the asphalt layer including longitudinal, transverse and vertical strains along with vertical stress. Finding the asphalt modulus as close as possible to the modulus that produces the in-situ measured responses plays a significant role in design and performance of pavement. Due to the inherent differences between response components under traffic loading in term of pulse shape and durations, evaluation of the associated frequencies for different response types is of utmost importance. Ulloa *et al.* [7] used theoretically-determined stress and strain pulses obtained from 3D-Move software [8] to investigate the impact of response type on the calculated frequencies in frequency domain. Results from this study showed that different predominant frequencies associated with longitudinal, transverse and vertical strains at the bottom of the HMA should be considered for the pavement analysis.

Reviewing the aforementioned literature reveals that relying on existing time-to-frequency conversion methods in time domain can lead to inaccurate frequency estimation. Considering the paradigm shift of computing the frequency in frequency domain rather than time domain, this paper focuses on the impact of such influential factors as vehicle speed, response type and analysis depth on the obtained frequencies through the field study. The present study was conducted at Integrated Road Research Facility (IRRF)'s test road

[1] Postdoctoral Fellow, University of Alberta, Markin/CNRL Natural Resources Engineering Facility, 9105 116th St., Edmonton, AB Canada T6G 2W2.

[+] Corresponding Author: E-mail abayat@ualberta.ca

Note: Submitted April 16, 2015; Revised October 6, 2015; Accepted October 8, 2015.

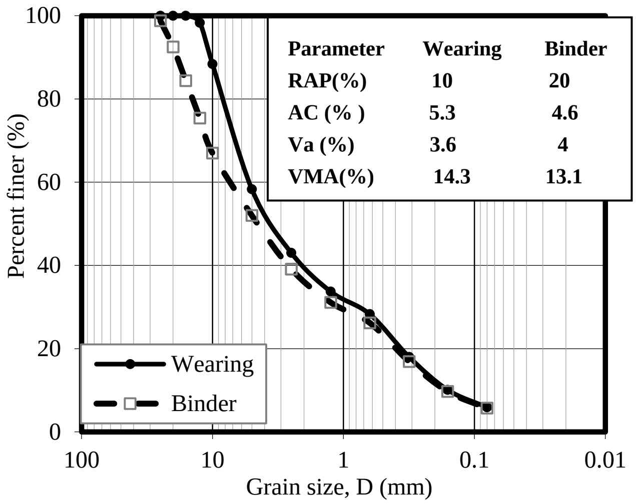

Fig. 1. Gradation and Physical Properties of HMA Mixes at IRRF.

facility in Edmonton, Alberta, Canada and several in-situ measured response pulses were analyzed to quantify the effect of using different approaches to |E*| prediction error.

Experimental Program

Integrated Road Research Facility (IRRF)

The IRRF's test road facility which connects the Edmonton Waste Management Centre (EWMC) to the Anthony Henday Drive (HWY 216) is located in the Northeast of the City of Edmonton, Alberta, Canada. The road is expected to open to traffic in the summer of 2015 with more than 500 garbage trucks transporting waste materials to EWMC every day. The pavement cross section consists of 90-mm wearing layer, 160-mm binder layer on top of a 450-mm granular base course (GBC) on top of clayey sand subgrade soil (SG). Fig. 1 shows the particle size distribution of the HMA mixes containing Reclaimed Asphalt Pavement (RAP) which were produced using PG 58-28 virgin asphalt binder. The wearing layer possessed a maximum aggregate size of 12.5 mm, while the maximum aggregate size was 25 mm for the binder layer.

There are two 20-m long monitoring sections in the test road approximately 100-m apart that are thoroughly instrumented to study the road response to traffic and environmental loading. Asphalt Strain Gauges (ASGs) and Earth Pressure Cells (EPCs) were used to collect the dynamic data at 500 Hz utilizing a high-speed CR9000X datalogger from Campbell Scientific Corp Canada®. Both control sections were similarly instrumented with ASGs at the bottom of the HMA layer in longitudinal, transverse and vertical direction named as ASG-L, ASG-T and ASG-V, respectively. As depicted in Fig. 2, one array of ASGs was laid along the outer wheelpath (OWP) in parallel with two other arrays at 600-mm lateral offsets to ensure the repeatability of the measurements. EPCs were also installed on the OWP and on the inner wheel path (IWP) at three different depths within the unbound layers.

Field Study

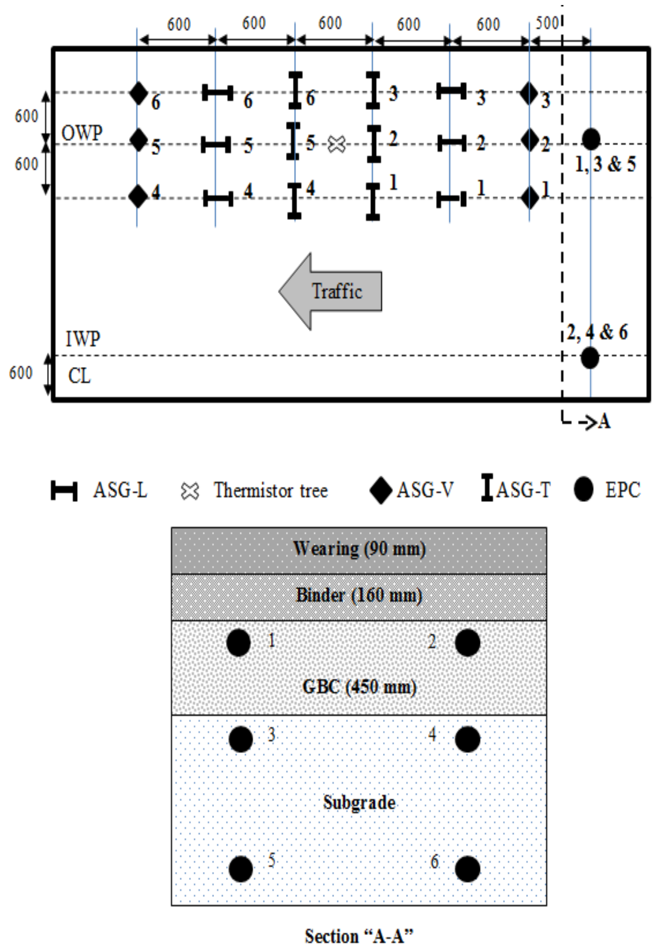

Fig. 2. Instrumentation Layout and Pavement Cross Section (all Dimensions are in mm).

A controlled vehicle testing was carried out at the IRRF' test road facility on August 14, 2014 using a two-axle dual tire single unit truck. The center-to-center distance between tires on the steering axle and rear axle was 2070 mm and 1920 mm, respectively. The rear axle was loaded to 40.69 kN and the steering axle weighed 25.00 kN. Besides, the tires' inflation pressure was measured equal to 870 kPa. The test runs were conducted at Section 2 of the IRRF starting from 2:30PM to 4:00PM and the HMA temperature at 20-mm depth below the surface varied between 34.1℃ and 37.6℃. Seven target speeds of 5, 10, 20, 30, 40, 50 and 60 km/hr were included in the experiment along the OWP. The runs were repeated at the seven target speeds in five replicates, resulting in a total of 7×5= 35 runs. Using an installed side-vehicle camera, videos were recorded during each run to check the wheelpath relative to OWP to ensure accuracy. The pressure measurement obtained from EPC (1), (3) and (5) as well as the strains recorded by ASG-V (2), ASG-L (2) and ASG-T (2) were considered for the analysis in this paper. It is noteworthy that this paper focuses on the response pulses collected under the dual tire on the rear axle of the vehicle.

Analysis of Loading Frequency

Fourier Representation of Pulses

Fourier transform of a function $f(t)$ in time domain can be expressed as $F(\omega)$ described in frequency domain using complex exponentials based on Eqs. (1) and (2) [9].

$$F(\omega) = \int_{-\infty}^{+\infty} f(t) e^{-i\omega t}\, dt \qquad (1)$$

$$e^{-i\omega t} = \cos(\omega t) - i \sin(\omega t) \qquad (2)$$

For the case of discrete data or a digital signal, Discrete Fourier Transform (DFT) can be used to determine the frequency content of the given signal according to Eq. (3).

$$F[m] = \sum_{n=0}^{N-1} f[n]\, e^{-i2\pi mn/N}, \qquad m = 0, 1, \ldots, N-1 \qquad (3)$$

where N is the total number of data points for a signal denoted as $f[n]$. On the other hand, FFT is an algorithm which facilitates the computation of the DFT especially in the computer programs. In this paper, frequency analysis of stress and strain pulses was performed using built-in FFT routine in Microsoft Excel®. The FFT routine in Microsoft Excel® restricts the number of data in the time-domain to a power of 2 including 1024 and 2048. Therefore, all the FFT analyses in this paper were performed based on 2048 number of data points collected at 0.002 s intervals. As the FFT outputs are in the form of complex numbers, the magnitude of the FFT outputs were calculated and then normalized with respect to the initial value.

Fig. 3(a) shows the typical measured stress (σ_v) pulses for the vehicle speed of 5 km/hr which were normalized relative to their peak values. The σ_v pulses clearly showed longer durations with the increase in depth. Fig. 3(b) depicts the corresponding normalized FFT magnitudes of the σ_v pulse in which frequency domain shapes were observed at different depths. It was found that the area under the generated frequency spectrums tended to decrease at deeper elevations. However, contributions of the higher frequencies were more noticeable for the σ_v on top of GBC layer in comparison to those of subgrade layer. Fig. 4(a) also shows the typical normalized strain pulses captured at the bottom of the HMA under the speed of 5 km/hr. While the strain in the longitudinal direction (ε_l) followed a compressive-tensile-compressive behavior, the transverse (ε_t) and vertical (ε_v) strains showed tensile and compressive behaviors, respectively. As presented in Fig. 4(b), the loading frequency spectrum associated with ε_l has a local maximum at approximately 1.5Hz, while ε_t and ε_v exhibited decreasing trends of FFT amplitude against frequency. The observed frequency spectrums confirm that the frequency calculation under moving load heavily depends on the response type, as it will be discussed in the next section.

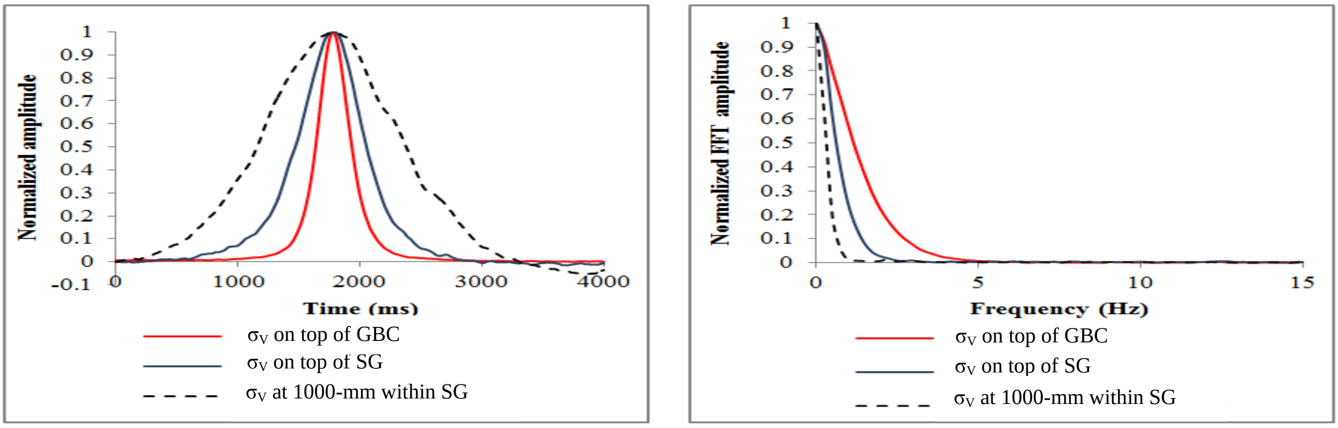

(a) (b)

Fig. 3. (a) Time Domain and (b) Frequency Domain of Measured Stress Pulses at 5 km/hr Speed.

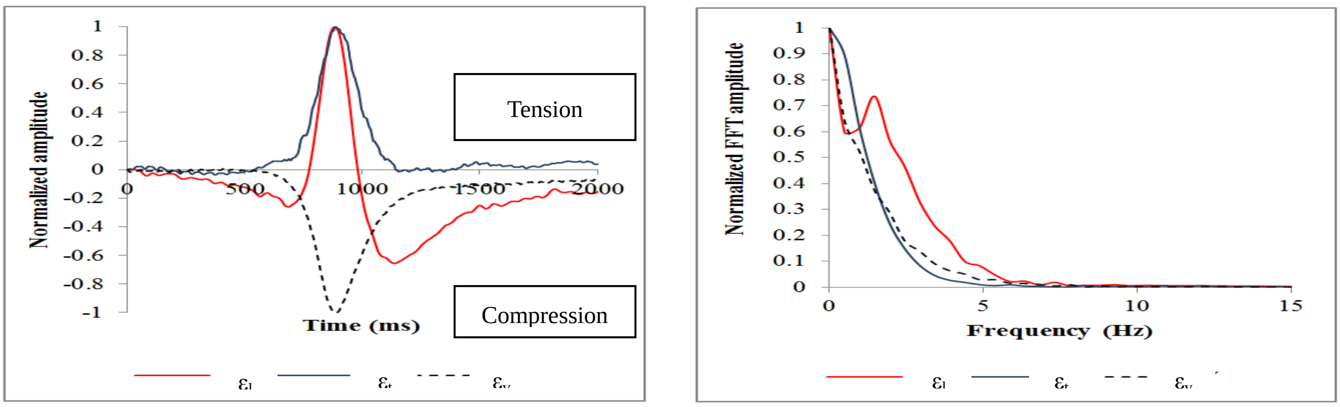

(a) (b)

Fig. 4. (a) Time Domain and (b) Frequency Domain of Measured Strain Pulses at the Bottom of the HMA at 5 km/hr Speed.

Table 1. Relationships between DF and Vehicle Speed.

Location	Regression Equation	R^2	S_e/S_y
Bottom of HMA	$DF\ (\varepsilon_l) = 1.165V^{0.45}$	0.97	0.20
	$DF\ (\varepsilon_t) = 1.158V^{0.40}$	0.97	0.18
	$DF\ (\varepsilon_v) = 0.607V^{0.50}$	0.99	0.07
Top of GBC	$DF\ (\sigma_v) = 0.482V^{0.62}$	0.99	0.05
Top of SG	$DF\ (\sigma_v) = 0.415V^{0.58}$	0.99	0.11
1-m within SG	$DF\ (\sigma_v) = 0.337V^{0.57}$	0.99	0.15

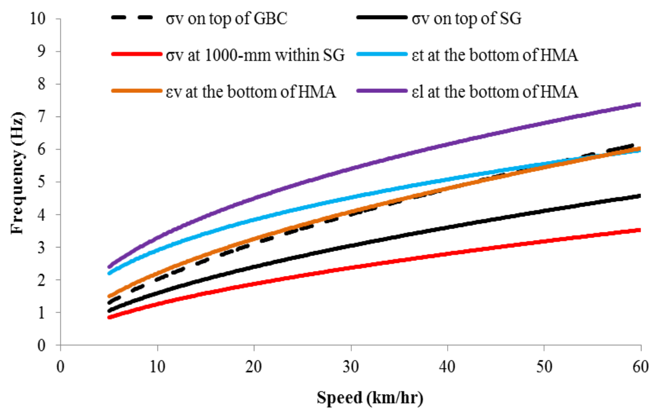

Fig. 5. Loading Frequency Determined from FFT for Different Response Types.

Effect of Response Type, Depth and Speed

To investigate the effects of contributing factors on the calculated loading frequency, frequency spectrums were analyzed for the six responses at each speed. Therefore, the dominant frequencies (DF) were extracted via finding the center of mass of the frequency spectrums as recommended by Al-Qadi *et al.* [10]. The extracted DF values were then averaged for the five replicates and plotted against the corresponding speeds as shown in Fig. 4. The fitted powerregression models are also represented in Table 1 where vehicle speed (V) in kilometer per hour is related to DF in Hertz. According to Table 1, the power regression models were highly accurate as the calculated R^2 values varied from 0.97 to 0.99, and S_e/S_y values for all models fell below 0.3.

Results from Fig. 5 confirm that DF for all stresses and strains increased at higher vehicle speeds, while the impact of speed on DF was more pronounced at lower depths. A reasonable agreement between DF values of ε_v at the bottom of the HMA and those of σ_v on top of the GBC was notable, implying the similarity between vertical stress and strain frequency at approximately the same depths. Besides, comparison between the corresponding DF values of σ_v at three different depths clearly illustrates that the difference between frequencies was more noticeable at higher speeds. From the analysis of DF values at the bottom of the HMA, it was found that the highest frequencies were associated with ε_l in which DF value as high as 7.5 Hz was calculated at 60 km/hr vehicle speed. On the other hand, the different DF of HMA strain pulses in three directions demonstrates that the anisotropic properties of HMA needs to be taken in to account when simulating flexible pavement response to moving loads.

Accuracy of Dynamic Modulus Prediction

Dynamic Mdulus from Laboratory

Due to the viscoelastic properties of HMA, |E*| strongly depends on the loading frequency and temperature. Laboratory tests were conducted to determine the dynamic modulus for both wearing and binder layers according to AASHTO TP79 [11]. To do so, Superpave gyratory compactor was used to prepare 150-mm-diameter by 170-mm-height cylindrical specimens representing the test road mixes. These samples were later cored and cut to 100-mm-diameter by 150-mm-height specimens for dynamic modulus test. Dynamic modulus tests were carried out at temperatures of -10, 4, 20 and 35℃ and frequencies of 10, 5, 2, 1, 0.5, 0.2, 0.1 and 0.01 Hz in order to develop the master curves based on AASHTO PP61 [12]. Fig. 6(a) depicts the constructed master curves, in which the binder course showed higher dynamic modulus compared to the wearing course considering its coarser aggregate gradation, lower bitumen content and higher RAP content. Additionally, the resulting shift factors are illustrated in Fig. 6(b). To later determine the |E*| at field temperature based on

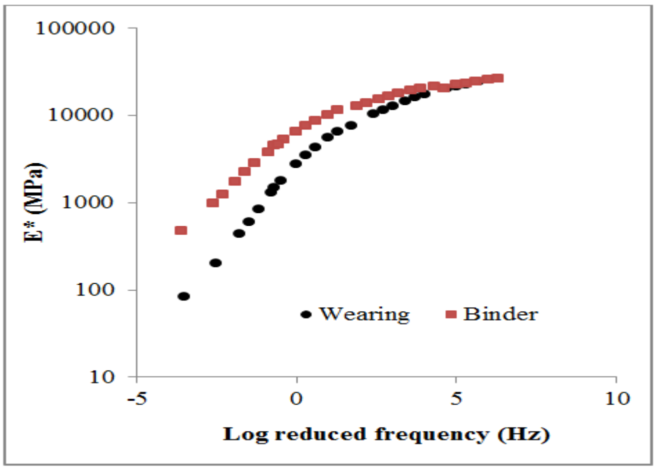

(a)

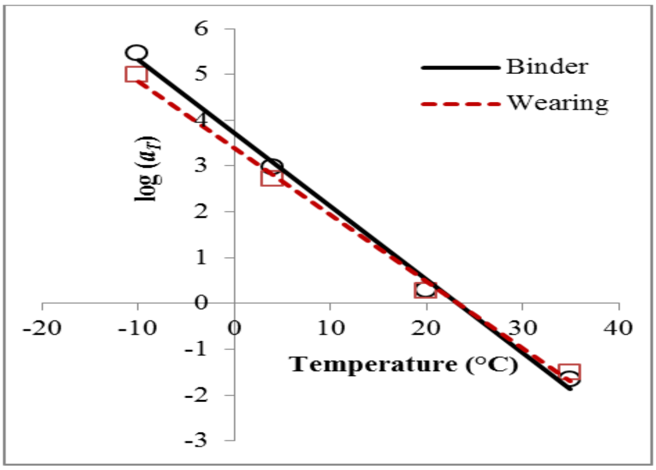

(b)

Fig. 6. (a) Master Curves at 20℃ Reference Temperature and (b) Shift Factors.

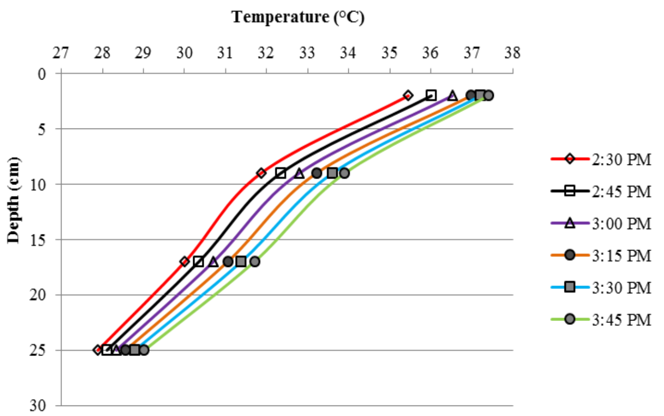

Fig. 7 Variation of Temperature at Different Depths within Pavement.

experimental master curves, temperatures from asphalt thermistors embedded at different depths within wearing and binder layers were used. Fig. 7 presents the temperature profile of the HMA obtained from the field thermistors during the controlled vehicle testing. The average temperature across wearing and binder layers were determined equal to 34℃ and 31℃, respectively. By applying the laboratory-established shift factors, the obtained |E*| values at the reference temperature of 20℃ were converted to the ones at the field temperatures for further analysis of $|E^*|$ variation at different frequencies.

Impact of Frequency Calculation Method on Dynamic Modulus

To evaluate the accuracy of FFT-calculated frequencies in terms of $|E^*|$ prediction and compare the DF values against other major frequency determination methods in time domain, different scenarios were defined as presented in Table 2. According to Table 2, four well-established frequency determination methods (cases 1 to 4) in the time-domain were selected from the literature and response pulse durations were converted to frequencies for each speed. Case 5 also demonstrates the adopted frequency calculation method in this paper which works according to the frequency spectra analysis. Among the defined cases, case 4 represents the current practice in the MEPDG for estimation of loading frequency. As presented in Table 2, the frameworks of frequency calculation in cases 1 to 4 consist of, firstly, finding the response pulse duration and, secondly, transforming it to frequency. Even though, the first step in cases 1 and 2 employ the actual in-situ measured pulse duration, cases 3 and 4 apply predictive equations to find the pulse duration. Moreover, pulse duration from in-situ measurements were converted to frequency using both $f = 1/t$ in case 1 and $f = 1/2\pi t$ in case 2 in an effort to compare the resultant frequencies. However, cases 3 and 4 require that time-to-frequency conversion be conducted using $f = 1/2\pi t$ and $f = 1/t$, respectively, as shown in Table 2. Since the recommended procedures in cases 3 and 4 rely on the stress pulse duration, the frequency calculations were performed focusing on σ_v on top of GBC in order to be consistent across all methods. In this analysis, the pulse duration was defined by doubling the elapsed time between the beginning of the stress pulse to its peak. It is worth noting that backcalculated layers' moduli of 210 MPa for GBC and 100 MPa for SG, obtained from Falling Weight Deflectometer (FWD) test conducted in early September 2014, were employed for calculations in case 4. Furthermore, the circular contact area was calculated by dividing the load on tire by the inflation pressure for finding the radius of contact area (a_c). Fig. 8 illustrates the relationships between stress frequency and speed for cases 1 to 5. It is clear that while not being very sensitive to speed increase, the frequencies obtained from case 2 were significantly lower than

Table 2. Frequency Calculation Scenarios Considered in this Study.

Methods	Loading Time	Loading Frequency	Parameters
Case 1	t=In-Situ Measured Pulse Duration	$f = \frac{1}{t}$ [2]	t = loading time (s) f = loading frequency (Hz)
Case 2	t=In-Situ Measured Pulse Duration	$f = \frac{1}{2\pi t}$ [4]	
Case 3	$Log\,(t) = 0.5\,h - 0.2 - 0.94\log(v)$ [13]	$f = \frac{1}{2\pi t}$	t = loading time (s) h = depth (mm) v = speed (mm/s) f = loading frequency (Hz)
Case 4	$t = \frac{L_{eff}}{17.6\,V}$ $L_{eff} = 2\,(a_c + Z_{eff})$ $Z_{eff} = \sum_{i=1}^{n-1}(h_i \sqrt[3]{\frac{E_i}{E_{SG}}}) + h_n \sqrt[3]{\frac{E_n}{E_{SG}}}$ [2]	$f = \frac{1}{t}$	t = loading time (s) L_{eff} = Effective length (in) V = speed (mph) a_c = radius of contact area (in) E_{SG} = modulus of subgrade n = number of layers h_n = thickness of the layer of interest (in) E_n = modulus of the layer of interest (psi) f = loading frequency (Hz)
Case 5	Loading Pulse in Time Domain	Frequency Spectra Using FFT	Not Applicable

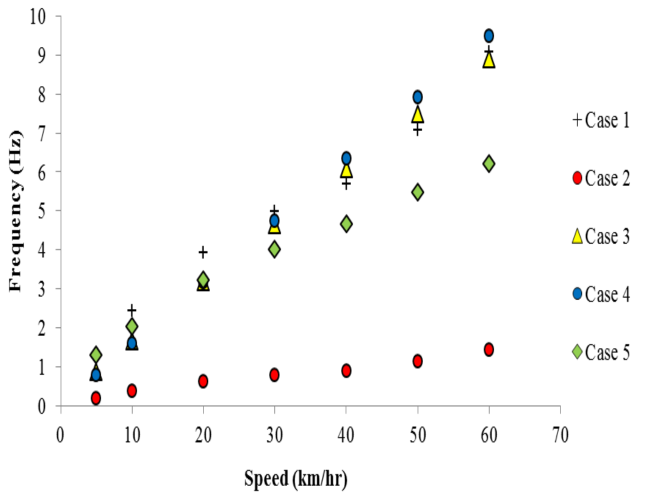

Fig. 8. Comparison of Stress Frequency vs. Speed in Different Methods.

those of the other cases. According to the literature, the ability of loading time prediction models and time-to-frequency conversion equations in prediction of field-measured pulses depends on their specific assumptions of time pulse shape and vehicular loading [6]. Therefore, this study confirmed that the underlying assumptions within case 2 lead to significant deviation from the rest of the reviewed methods. It is appropriate to note that even though the proposed approximation methods in cases 3 and 4 yielded incompatible loading time values, both methods' estimated loading frequencies were in good agreement with those of case 1 due to their particular time-to-frequency conversion approaches. In addition, the FFT-calculated frequencies were generally lower than the results from case 1 and larger than those of case 2, especially at vehicle speeds of 30 km/hr and higher. The observed overestimation and underestimation can be partially attributed to the facile approach used within cases 1 and 2 for direct time-to-frequency conversion. This is in agreement with the findings of Al-Qadi *et al.* [6] for speeds of 8, 24 and 40 km/hr and stress pulses at 140 and 190-mm depths at the Virginia Smart Road.

In order to translate the effect of calculated frequencies on the |E*|, it is necessary to input the calculated frequencies in the laboratory-determined HMA master curve. Therefore, for each of the cases, |E*| values were extracted from the wearing and binder layers' master curves at different obtained frequencies. Then, by calculating the weighted average of the extracted |E*| of the two layers, a single |E*| was generated to represent the stiffness of a combined HMA layer at any frequency. Using the weight factors of 0.36 for wearing and 0.64 for binder based on each layer thickness, E_{com} was derived at each frequency for further comparisons. On the other hand, estimation of linear elastic modulus of HMA based on the in-situ measured stresses, as depicted in Fig. 9(a), can provide an approximate benchmark for comparing the |E*| values. To pursue this purpose, simulation of the test section response to vehicle load was conducted using KENLAYER [1] by estimating the linear elastic moduli of HMA (E_{est}) until the predicted σ_v on top of GBC converges to its in-situ measured value by ±1% at each speed. During the analysis of E_{est}, the wearing and binder layers were combined and assumed as a single HMA layer, while other

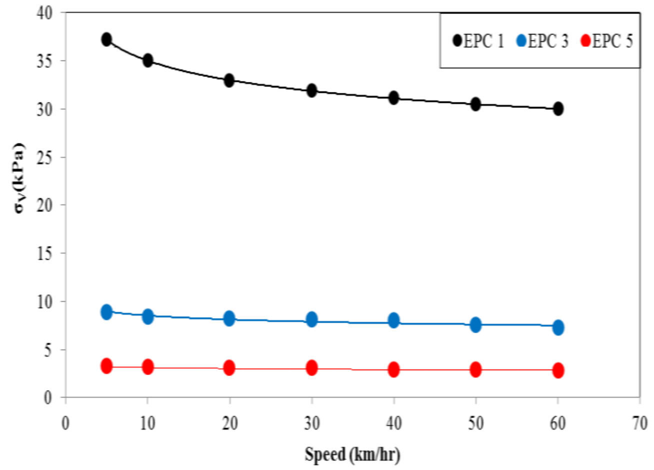

(a)

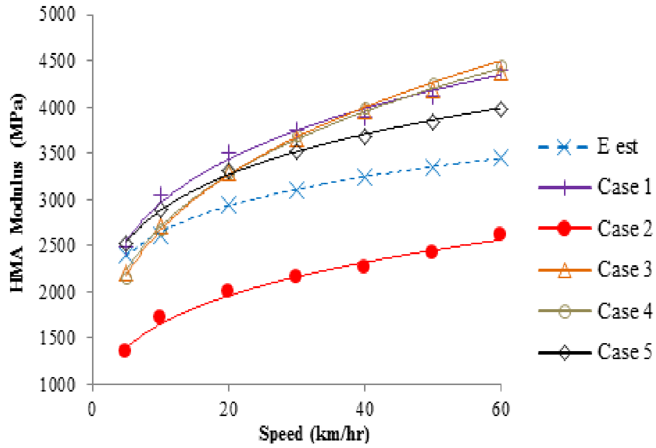

(b)

Fig. 9. (a) Variation of σ_v on Top of GBC and, (b) E_{est} and E_{com} vs. Speed.

parameters such as GBC modulus (210 MPa) and subgrade modulus (100 MPa) were considered constant. Fig. 9(b) shows the variation of estimated E_{est} to match σ_v on top of GBC and E_{com} for the five frequency calculation cases against speed. Results showed that magnitudes of E_{com} of case 2 were noticeably lower than E_{est} and E_{com} of other cases. As expected, the E_{com} of cases 1, 3 and 4 fairly changed within the same range against speed and were larger than those of case 5 for speeds of 20km/hr and higher. The effectiveness of E_{com} of the five cases with respect to E_{est} was evaluated in terms of percentage of prediction error, PPE:

$$PPE = \frac{E_{com} - E_{est}}{E_{est}} \times 100 \quad (4)$$

Fig. 10 depicts the PPE of the E_{com} for different cases in which positive values contribute to over-estimated E_{com}, whereas negative values contribute to under-estimated E_{com}. The distribution of the PPEs for the five cases suggests that case 5 had the lowest median and possessed less variation in comparison to other cases. Almost similar patterns were observed for cases 3 and 4 and both methods resulted in a wide range of PPE including over-estimated and under-estimated values. Although, the median of PPEs in case 1 was fairly closed to those of cases 3 and 4, the PPEs of case 1 varied within a more limited range. This is supported by the fact that the

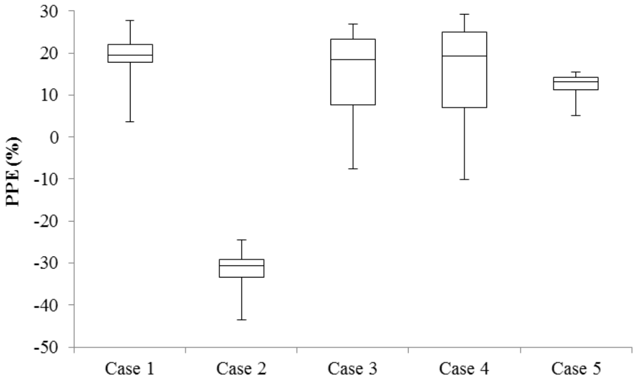

Fig. 10. Comparison of Modulus Prediction Errors for Different Approaches.

standard error of PPEs in case 1 (2.8 %) was less than that of PPEs in case 3 (4.8%) and case 4 (5.4%). In overall, case 2 exhibited the highest PPEs with values as high as 44. Therefore, the use of FFT to calculate DF may generally result in more efficient prediction of the HMA dynamic modulus over the tested range of speeds. Moreover, the lowest standard error of PPEs in case 5 (1.3%) amongst all considered cases confirms that case 5 is less sensitive to speed variation compared to four other methods.

Conclusion

This paper investigated the use of FFT for calculation of frequency associated with longitudinal, transverse and vertical strains at the bottom of the HMA as well as the vertical stress at different depths within unbound materials. In this study which was conducted at the IRRF's test road facility, responses from several controlled vehicle testing performed at different speeds were utilized and relationships were developed to approximate dominant frequencies as a function of vehicle speed. The observed differences between obtained dominant frequencies revealed that longitudinal strain possessed the highest frequencies in comparison to transverse and vertical strains. Besides, the calculated frequencies noticeably decreased at deeper elevations, while a reasonable agreement between frequencies of vertical strain at the bottom of the HMA and vertical stress on top of the GBC was observed. Focusing on the vertical stress response on top of GBC, results from FFT method were compared to those of four other widely-used time-domain frequency calculation methods. Finally, comparisons between the |E*| determined from five different cases with respect to the estimated modulus matching in-situ measured vertical stresses showed that FFT yields more accurate and reliable moduli.

Acknowledgements

The authors gratefully appreciate the assistance of Alberta Transportation, Alberta recycling, and The City of Edmonton who provided financial and in-kind support for the construction and instrumentation of the IRRF's test road. Alberta Transportation is also acknowledged for conducting the FWD tests for this study. The close cooperation of Tetra Tech EBA FWD test crews during testing is also greatly appreciated.

References

1. Huang, Y.H. (1993). *Pavement analysis and design*. 2nd Edition, Prentice Hall, Inc., Upper Saddle River, NJ, USA.
2. ARA, Inc. (2004). Guide for Mechanistic–Empirical Design of New and Rehabilitated Pavement Structures. Final report, NCHRP Project 1-37A. Transportation Research Board of the National Academies, Washington, DC, USA. http://www.trb.org/mepdg/guide.htm.
3. Dongre, R., Myers, L., and D'Angelo, J. (2006). Conversion of testing frequency to loading time: Impact on performance predictions obtained from the ME Pavement Design Guide. Presented at the 85th Transportation Research Board Annual Meeting (Paper No. 06-2394), Washington, DC, USA.
4. Ferry, J. D. (1980). *Viscoelastic properties of polymers*. John Wiley & Sons, New York, New York, USA.
5. Odemark, N. (1949). *Investigations as to the Elastic Properties of Soils and Design of Pavements According to the Theory of Elasticity*, Meddelande 77, Staten Vaeginstitut, Stockholm, Sweden.
6. Al-Qadi, I.L., Elseifi, M.A., Yoo, P.J., Dessouky, S.H., Gibson, N., Harman, T., and Petros, K. (2008). Accuracy of current complex modulus selection procedure from vehicular load pulse: NCHRP project 1-37a mechanistic-empirical pavement design guide. *Transportation Research Record*, 2087(1), pp. 81-90.
7. Ulloa, A., Hajj, E.Y., Siddharthan, R.V., and Sebaaly, P.E. (2012). Equivalent Loading Frequencies for Dynamic Analysis of Asphalt Pavements. *Journal of Materials in Civil Engineering*, 25(9), pp. 1162-1170.
8. Siddharthan, R.V., Yao, J., and Sebaaly, P.E. (1998). Pavement strain from moving dynamic 3D load distribution. *Journal of Transportation Engineering*, 124(6), pp. 557-566.
9. Wong, M.W. (2011). *Discrete Fourier Analysis*. Springer Science & Business Media, Birkhäuser, Ontario, Canada.
10. Al-Qadi, I.L., Xie, W., and Elseifi, M.A. (2008). Frequency determination from vehicular loading time pulse to predict appropriate complex modulus in MEPDG. *Journal of the Association of Asphalt Paving Technologists*, 77, pp. 739-772.
11. AASHTO (2009). Determining the Dynamic Modulus and Flow Number for Hot Mix Asphalt (HMA) Using the Asphalt Mixture Performance Tester (AMPT), *AASHTO TP79-09*, American Association of State Highway and Transportation Official, Washington, DC, USA.
12. AASHTO (2009). Developing Dynamic Modulus Master Curves for Hot Mix Asphalt (HMA) Using the Asphalt Mixture Performance Tester (AMPT), *AASHTO PP61-09*, American Association of State Highway and Transportation Official, Washington, DC, USA.
13. Brown, S.F. (1973). Determination of Young's modulus for bituminous materials in pavement design. *Highway Research Record*, (431), pp. 38-49.